Article

Design of a RGB-Arduino Device for Monitoring Copper Recovery from PCBs

Joan Morell [†], Antoni Escobet [†] ⬤, Antonio David Dorado *,[†] ⬤ and Teresa Escobet [†] ⬤

Department of Mining, Industrial and ICT Engineering, Universitat Politècnica de Catalunya—BarcelonaTech (UPC), 08242 Manresa, Spain
* Correspondence: toni.dorado@upc.edu
† These authors contributed equally to this work.

Abstract: The mobile phone industry, one of the fastest advancing sectors in production over the last few decades, has been associated with a high e-waste generation rate. Simultaneously, a high demand for the production of new electronic equipment has led to the scarcity of certain metals. In this context, many recent studies have focused on recovering certain metals from e-waste through the use of bioprocesses. Such recovery processes are based on the action of microorganisms that produce Fe(III) as an oxidant, in order to leach the copper contained in printed circuit boards. During the oxidation-reduction reaction between Fe(III) and metallic Cu, the color of the solution evolves from an initial reddish color, due to Fe(III), to a bluish-green color, due to the oxidized Cu. In this work, a hardware-software prototype is developed, through which the concentrations of the key analytes—Fe(III) and Cu(II)—can be determined in real time by monitoring the color of the solution. This is achieved through the use of a non-invasive system, taking into account the aggressiveness of the solutions used for the bioprocessing of electronic components. In the work presented herein, the evolution of the solution color during the bioprocessing of two different types of waste (i.e., electric cable and mobile phones) is analyzed and then compared with the results obtained for pure metallic copper. The results are validated through comparison of the predicted results with the outcomes of conventional procedures, including offline sampling and analysis of Cu(II) and Fe(III) through atomic absorption and UV-VIS spectroscopy, respectively. The developed monitoring system allows an algorithm to be designed that can fit the evolution of analyte concentrations without the need for sampling or the use of complex, tedious, and expensive analytic techniques. It is also worth noting that the monitoring system is not in direct contact with the solution (which is highly aggressive for the processing of electronic equipment), making the system more durable than classic sensors that must be submerged in the solution. The real-time nature of the obtained information allows for the development of control actions and for corrective measures to be taken without affecting the biomass involved in the process.

Keywords: copper recovery; mobile phone waste; bioprocess optimization; chemical reactions; real-time monitoring system; color sensing; non-invasive sensors

1. Introduction

The exponential increase in electric and electronic equipment (EEE) over the last few decades has led to an alarming level of consumption of natural resources and the continuous generation of electronic waste (e-waste). Global e-waste statistics indicate that the total amount of e-waste generated globally increased from 44.6 million tons in 2014 to 53.6 million tons in 2019, and it has been estimated that annual e-waste generation will increase to 74 million tons by 2030 [1]. Unfortunately, only 17.4% of the world's e-waste was recorded as being recycled in 2019, leaving 82.6% unaccounted for. This recovery rate was not a significant improvement over that in 2014 (17%), indicating that measures to increase global e-waste recycling rates have not been able to compete with

the increase in e-waste [1,2]. On the other hand, e-waste is considered an 'urban mine', as it contains precious metals (e.g., gold, silver, copper, platinum, palladium, ruthenium, rhodium, iridium, and osmium), critical raw materials (e.g., cobalt, indium, germanium, bismuth, and antimony), and non-critical metals, such as aluminum and iron. For this reason, within the circular economy paradigm, e-waste has been considered as an important source of secondary valuable raw materials [3].

Of all the EEEs, waste mobile phones (WMPs) are the fastest-growing among all kinds of waste; however, their collection and recycling rates remain almost insignificant (e.g., under 10%) [4,5]. At present, the WMP recycling rate is low [6]; even for countries with sophisticated WEEE collection and recycling systems such as Switzerland and Germany. As a result, the global supply of metals may not be sufficient to satisfy the ever-increasing demands of the electrical and electronic equipment (EEE) industry [7].

Waste mobile phones typically consist of many materials, including plastic, printed circuit boards (PCBs), screens, magnets, vibrators, LED backlights, steel, and batteries. Four key components can be distinguished in a mobile phone: the printed circuit board (PCB), the display unit, the battery, and the case. Gu et al. [7] conducted a bibliographic review of all articles published after Jan 2005 and before May 2019 focused on "recycling or recycle or recover or material recover" on "waste mobile phone or spent mobile or phone or cell phone or mobile phone". They retrieved a total of 68 publications, over half of which the reported methods for the recovery of metals from WMP PCBs and 19 from WMP batteries. This is because the most valuable components in mobile phone e-waste are the printed circuit boards (PCB) and the lithium-ion batteries (LIBs), due to their high precious and base metal content.

Without considering batteries, Singh et al. [8] analyzed twenty types of cellular and smartphones and concluded that, on average, the weight of the PCB (including the metallic wire) versus the total weight of a WMP ranges between 10–30%. PCBs are the most complex part in e-waste, including (apart from the support) integrated circuits and other electronic components containing approximately 60 kinds of elements: 28–30% ceramics, 27–30% organic materials, and 34.9% metals [9]. The metallic composition varies according to the type of mobile phone. By analyzing the metal content of basic and smartphones manufactured between 2001 and 2015, Singh et al. [10] identified 19 metals, with cobalt (Co), tin (Sn), chromium (Cr), copper (Cu), and zirconium (Zr) being the most abundant.

PCBs contain up to 66 different chemical elements, some of which are considered hazardous. The challenge of protecting the environment has spurred the need to develop and adapt existing sustainable and cost-effective technologies to extract these metals from e-waste. Among these elements, copper is one of the most valuable metals to recover, due to the high demand for it in the fabrication of new electronic devices and components [11]. Copper (Cu) is classified as "cross-cutting", defined by the World Bank as essential in energy and clean storage technologies (WBG, 2020). Copper remains one of society's most widely used metals, playing a vital role in electronic devices, vehicles, and electrical power generation, among many other applications. This high demand is due to the numerous important uses facilitated by its malleability, ductility, conductivity (of both heat and electricity), and capacity to withstand corrosion.

Methods used to recover metals from e-wastes can be grouped into physical, chemical, thermo-chemical, electrochemical, pyro-metallurgical, hydrometallurgic, and bio-metallurgical methods, or a combination of them [12]. Many papers have recently reviewed techniques for recovering and processing copper, as well as proposing improvements with the objective of reducing the consumption of energy, the time needed, or the consumption of corrosive and hazardous leaching agents, among other aspects ([13,14]). Biohydrometal-lurgic processes have been developed as an alternative technology for recovering metals. These techniques are based on the extraction of metals by means of the metabolic activity of bacteria or metabolic compounds. Such biologically assisted degradation of waste has a high potential as a recycling technology, due to the low environmental impact, operational costs, and energy requirements [15]. Microbially mediated extraction procedures are more

environmentally friendly than traditional physicochemical approaches [16]; this is because biological recovery is usually performed under ambient conditions, significantly reducing the required energy in comparison to pyro-metallurgical extraction, as well as reducing harmful gas emissions. Moreover, the metabolic products formed during bioleaching are harmless, hence avoiding the need for expensive palliative measures to prevent environmental pollution and processing risks. Consequently, biological recovery methods result in both lower operating investment and reduced environmental impact [15].

The typical method for biological Cu recovery consists of four steps (depicted in Figure 1), as previously described in [17,18]. The first stage consists of creating the leaching agent through the use of bacteria, which oxidizes Fe(II) to Fe(III) under controlled pH and dissolved oxygen concentration conditions in a fixed-bed reactor. *Acidithiobacillus ferrooxidans*, which operates under extremely acidic conditions (e.g., pH of 1.5), is the most commonly utilized bacteria for oxidation of Fe(II) to Fe(III). In the second stage, biomass is recovered from Fe(III) solution produced to avoid the presence of microorganisms in the following steps. Subsequently, the leachate is brought into contact with the e-waste under aggressive acid conditions (pH < 1.5), guaranteeing optimal liquid–solid contact (it is worth noting that, at this point, the e-waste has been previously processed to decrease the size and favor the contact). The final stage consists of selective recovery of the metal from the resulting solution. The resulting Fe(II) solution is then regenerated biologically and returned to the first stage to produce the Fe(III) needed to continue the process.
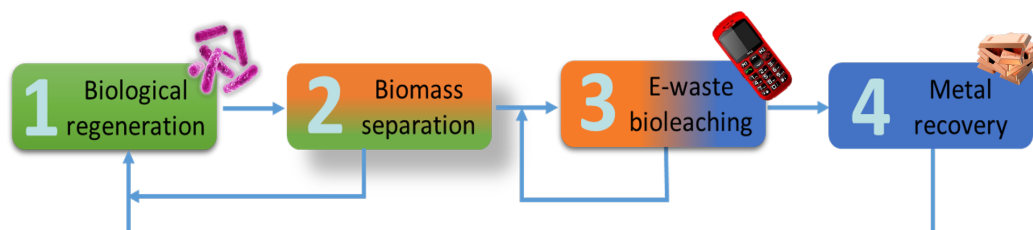
Figure 1. Schematic of the multi-step process for metal recovery from PCBs: (1) Preparation of the leaching agent in presence of the biomass; (2) Biomass separation; (3) Cu extraction from e-waste pre-processed by the leaching process; and, (4) metal recovery from the liquid solution.

One of the most important challenges regarding the correct operation of the process is to develop control strategies guaranteeing steady and optimal operation conditions. For this purpose, the monitoring of some key variables, such as the Fe(II), Fe(III), and Cu(II) concentrations, is indispensable. In most laboratory applications, samples are periodically collected and these concentrations are determined through offline laboratory analysis, resulting in a long response time and potentially hindering rapid application of the correct measure. Although there are specific online sensors that can be used for this purpose, they are usually expensive and must be submerged into the leaching solution, which is considered highly aggressive for such sensors as dissolving metals from electronic components is the final purpose of the process.

As discussed in Section 3 and depicted in Figure 1, during the dissolution of metals presented in the e-waste, the color of the solution changes from green to red and blue, according to the concentrations of the reagents and products. Taking advantage of this property, in this paper, we present a low-cost monitoring technique based on analysis of the signals captured by a digital RGB (red–green–blue) sensor which can automatically detect red, green, blue, and infrared signals in its field of view. This technique has been explored by Madriz et al. [19], who used a smartphone to measure the color of a reaction, allowing for its evolution to be correlated with kinetic parameters. The proposal presented herein is designed as a more economic approach. An interesting review of novel approaches for colorimetric measurement in analytical chemistry has been recently published by Fernandes et al. [20], who highlighted the need for an efficient light emitter and promoted the use of a light-emitting diode (LED) for this purpose. They also pointed out that the light spectrum will affect the colorimetric results and, so, a comparison of

the absorbance spectrum of the colored substance against possible LED emitting spectra is essential to determine the linear relationship between concentration and the analytical signal(s). Numerous publications have evaluated the capability of RGB sensors for colorimetric determination ([21–24]). All of these studies have used a light-emitting diode (LED) and an RGB sensor connected to a single-board Arduino for data acquisition and manipulation, which achieved satisfactory results. In the described experiments, color detection was performed by assessing samples stored in appropriate containers. Another interesting review of different methods for color measurement, applied to amber-colored liquid cases, has been published [25]. This review demonstrated that existing color measurement techniques can determine the color, according to relevant standards and color scales, and the authors suggested putting increased effort into determining an optimized method or technique for color measurement of liquids, thus expediting the development of a portable device that can measure color accurately.

The work presented herein details the design of a low-cost device for real-time monitoring of the progress of the chemical reaction involved in the recovery of copper from e-waste through the use of microorganisms, both allowing for improvement of the process and providing a more sustainable approach than conventional ones. The device is both hardware- and software-based: the hardware consists of a color sensor and an Arduino, which carries out pre-processing and transmits the data to a computer. The use of such a system, which allows for data acquisition, signal processing, and color monitoring in real-time, provides a potential tool for use as a research component to improve knowledge regarding the use of bioprocesses for the recovery of metals from e-waste; furthermore, this approach is also applicable to other hydrometallurgic process based on the solubilization of metals through direct contact between e-waste and leaching agents.

2. Materials and Methods
2.1. Experimental Designs and Analysis Methods

In this study, the experiments are designed for measuring the progress of the oxidation of metallic copper by Fe(III) which in turn is reduced to Fe(II), according to the reaction (1):

$$Cu^0 + 2Fe^{3+} \longrightarrow Cu^{2+} + 2Fe^{2+} \tag{1}$$
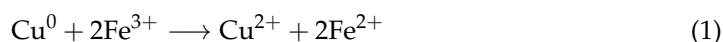
The oxidant solution was prepared by dissolving 34.4 gr of $Fe_2(SO_4)_3$ with a purity of 75% in distilled water at pH 1.5. The pH is adjusted by 10% concentrated sulfuric acid. Copper was obtained from three different sources: Metallic copper, electrical cable (EC) and phone boards (PB). Figure 2a,b show the original e-waste material and the crushed material used in the experiments exp-EC and exp-PB, respectively.


(**a**)   (**b**)
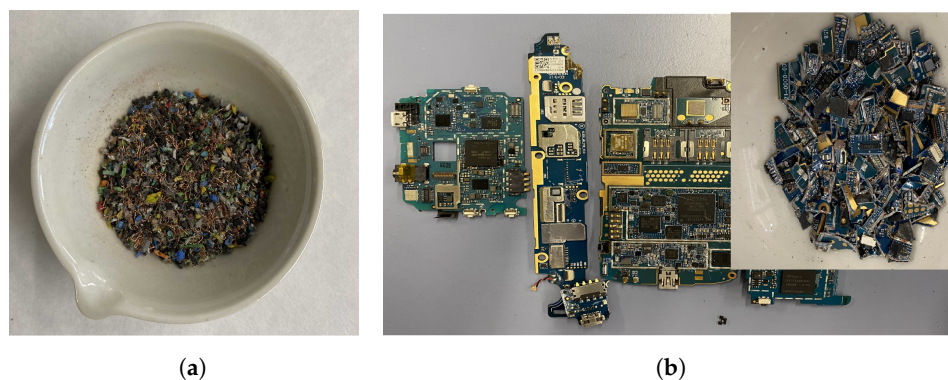
Figure 2. Material used in the experiments. (**a**) Crushed electrical cables. (**b**) Phone boards (original and crushed).

In order to determine the content of copper in the mobile phone PCB samples and in the electrical cables, wet digestion was performed. For this purpose, approximately 0.1 g

of the solid sample and 10 mL of HNO_3:HCl (3:1) were introduced into an appropriate container. The samples were subsequently introduced into a microwave apparatus (Microwave System, Millestone, Italy) at 150 °C for 30 min. Then, the solution was filtered at 0.45 μm, in order to separate the liquid from the solid particles that could not be completely digested. Finally, an appropriate dilution was required to analyze the Cu(II) concentration by atomic absorption spectroscopy (AAS). The repeatability of the analysis was determined by taking 5 measurements [26].

Color characterization was carried out by comparing the values obtained by the sensor with the concentrations of Fe(III) and Cu(II) present in the solution, determined using an ultraviolet–visible (UV-Vis) spectrometer and atomic absorption spectroscopy (AAS), respectively. UV-Vis spectroscopy was carried out to analyze the Fe(III) concentration by measuring the intensity of light that passes through the sample and comparing it to the light intensity without the sample. In this work, Fe(III) concentrations were measured using a UV-Vis spectrometer (Lambda 25, PerkinElmer, United States), following the standard colorimetric method that uses salicylic acid as a chelating agent [27]. Samples analyzed by UV-Vis were previously filtered at 0.45 μm, in order to avoid solids remaining in the suspension which could lead to erroneous results in the analysis. Subsequently, as the linearity of Fe(III) is between 0 and 40 mg/L, the samples were diluted with distilled water at pH 1.8 and mixed with a solution of salicylic acid 5% (*w/v*) in ethanol. The pH level of the distilled water (1.8) was adjusted by adding sulfuric acid at 10% concentration (*v/v*). The reaction between Fe(III) and salicylic acid is as follows:

$$Fe^{3+} + 2C_7H_6O_3 \longrightarrow [Fe(C_7H_5O_3)_2]^+ + H^+ \qquad (2)$$
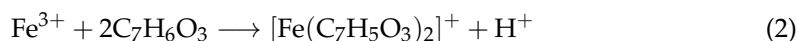
In the final step, samples were analyzed with UV-Vis spectroscopy, with the maximum wavelength of Fe(III)-SA complex being 527 nm, having an absorbance of 0.458 and a molar extinction coefficient of 1.8×10^{-3} M^{-1} cm^{-1}. On the other hand, the rest of the metal elements that can be found in liquid samples were analyzed by atomic absorption (AA). The AA spectrometer used in this study was a Solar S2 (Thermo Fisher Scientific, United States). Samples were also filtered at 0.45 μm and diluted according to the linearity of the metal response.
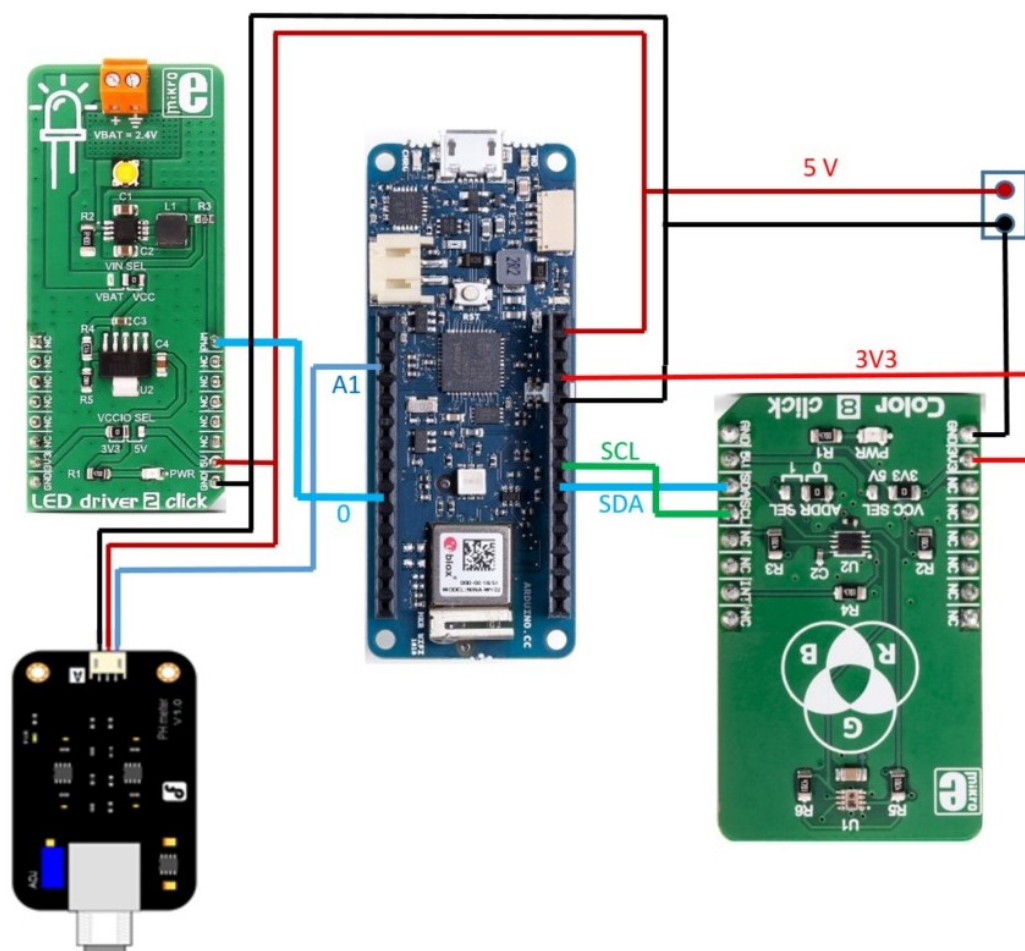
2.2. Developed Measurement System

Figure 3 shows the components and wiring connections of the developed system for measuring the color evolution in the copper recovery process. It consists of an Arduino MKR1010 board for control and data processing, a color sensor board [28], an LED driver [29], and a pH sensor [30]. As can be seen from Figure 3, the color sensor is connected to the serial Inter-Integrated Circuit (I2C) bus, the LED driver is connected to a digital output pin (0), and the pH sensor is connected to an analog input pin (A1). The I2C is a two-wire bus that includes serial data (SDA) and serial clock (SCL) lines [31].

The color sensor board utilizes an RGB-IR color sensor (BH1749NUC) to obtain the color signal, the characteristics of which have been previously described in [32]. This sensor senses Red (R), Green (G), Blue (B), and Infrared (IR) signals and converts them to digital values. It includes four independent photo-diodes for detection of the separate wavelengths (i.e., red, blue, green, and infrared), as well as three independent A/D converters which are used to digitize the color intensity in 16-bit resolution. One of the converters—which is otherwise used for the blue light—is internally multiplexed with the IR photo diode. It also incorporates an IR-cut filter, which is used to block the portion of the light in the IR spectrum which can interfere with the readings of the photo-diodes used to sense the red, green, and blue components of the light.

The color sensor includes two configuration parameters: Transimpedance amplifier gain (TIA) and measurement time. The first—TIA—is available for both the RGB and IR channels, and allows for amplification of the signal by 1 or 32. The latter—measurement time—should be selected from 35 ms, 120 ms, or 240 ms. Note that, when using the highest gain ratio in combination with the longest measurement time, it is possible to achieve a

resolution of 0.0125 lux/count. In this application, we configured the sensor with a TIA of 1 and a measurement time of 240 ms. The color and IR conversion results are provided at the output registers in MSB/LSB format.


Figure 3. Components and wiring connections of the developed measurement system.

For the experiment, the color sensor was installed in front of the reactor vessel. The vessel where the copper is recovered consists of a transparent plastic cylinder with a height of 33 cm, external diameter of 11 cm, internal diameter of 8 cm, and a total volume of 1.6 L. It was located in the laboratory under variable illumination conditions. To prevent external light variations, a white LED of 101 lm at 25 °C [33] was placed in front of the RGB sensor. Both the color sensor and LED boards were placed in the plastic piece shown in Figure 4a, which was obtained using a 3D printer. This piece was designed to enclose both circuit boards to protect them from the corrosive environment, ambient light isolation, and to keep them held up to the vessel environment, as shown in Figure 4b.

Data Acquisition and Control System

For the developed measurement system, an Arduino was used for light-emitting diode switching, as well as reading, pre-processing, and transmitting the color sensor data to the computer. As described in Algorithm 1, the program works cyclically and begins illuminating the liquid solution by switching on the white LED. After a pre-determined time, I2C communication is established between the Arduino and the color sensor board, which waits for data transmission. In this application, a total of 10 consecutive measurements are recorded. Then, the LED is switched off and data pre-processing is started.

(**a**)   (**b**)
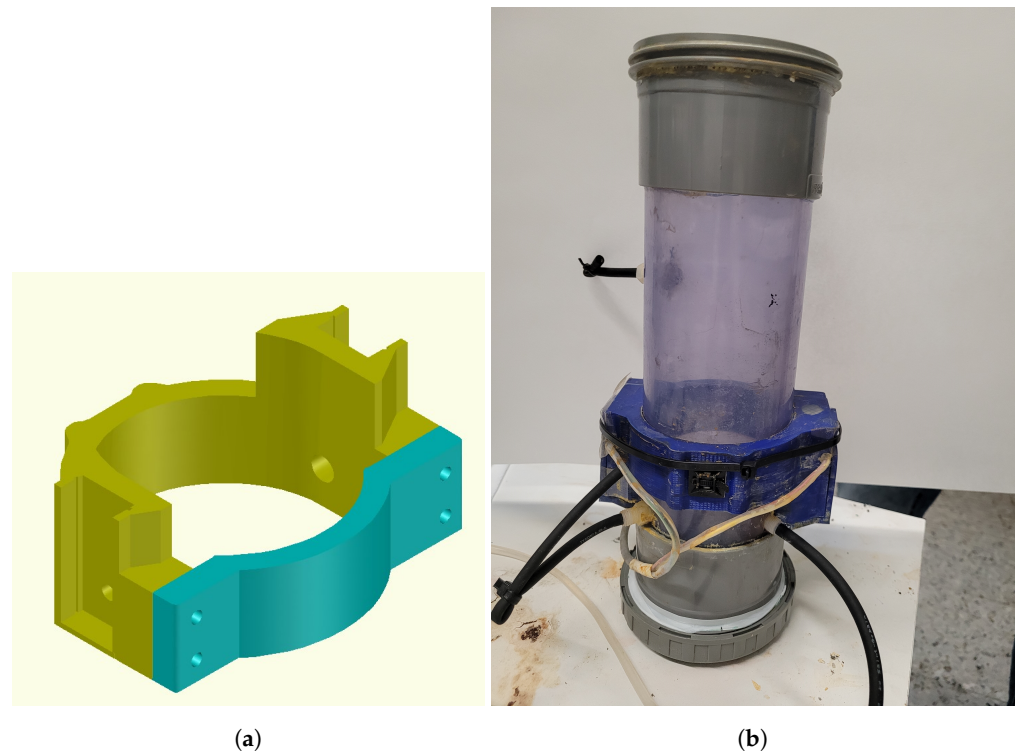
Figure 4. Designed plastic piece for enclosing LED and sensor color boards. (**a**) 3D design for printing. (**b**) Location of the designed piece in the vessel.


Algorithm 1 Data acquisition and data processing

1: Wait for the start command from the control center.
2: Open the LED and wait for one second.
3: Send request to the RGB-IR color sensor and wait for the response (about 240 ms).
4: Read the received data (8 bytes of information).
5: Extract and remove the four least significant bits.
6: Classify the data according to its attributes (in our case, the data are classified into four categories: red, green, blue and infrared).
7: Store the data in column/row format (where each column represents one attribute and each row contains a record).
8: Steps (3)–(7) are repeated 10 times.
9: From the 10 data for each class, the maximum and minimum are removed, in order to avoid spurious values.
10: The remaining eight values are used to calculate the mean arithmetical values, in order to reduce the random noise of measurements.
11: The processed data are packed and sent to the computer.

Data pre-processing begins with unpacking the collected samples, according to the communication protocol, and removing the four least significant bits for randomness extraction, giving color intensity data with 12-bit resolution. Next, the raw data are classified into four classes, in terms of the RGB-IR color sensor measurement reading. Finally, in order to transform the raw data into refined information assets, cleaning of the data first takes place. The data in the four classes (i.e., red, green, blue, and infrared) to be transferred to the computer are determined by averaging the values of each class after removing the maximum and minimum values.

A PC application was designed using the LabWindows/CVI platform, which stores, processes, and monitors the transmitted color data. This monitoring system allows the user to establish a connection with the Arduino, watch in real-time the RGB-IR data received,

and process the data for color reproduction and display; see Figure 5. It also controls when data acquisition is started and stopped, the LED intensity, and the sampling time.
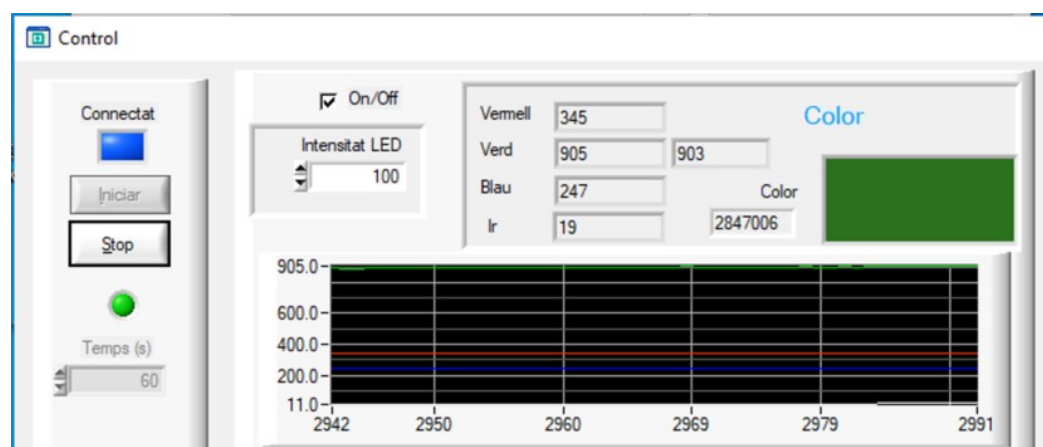
Figure 5. Developed monitoring system.

### 2.3. Sensor Calibration and Color Reproducing

One of the objectives of the developed sensor is to capture and emulate the color of the chemical reaction. For this purpose, the color evolution in the vessel was first observed using a smartphone camera. The five images in Figure 6 show the color evolution in the vessel over the course of one of the experiments. The initial color of the solution was brown, due to the presence of Fe(III). The color of the solution gradually changed from brown to blue, in correspondence with the oxidation of copper by Fe(III) ions which, in turn, were reduced to Fe(II), according to Equation (1).

Figure 6. Color evolution at different stages of the redox reaction.

The red, green, and blue lines in the upper part of Figure 7 denote the RGB sensor values in real-time for this experiment. The data were recorded with a sampling time of 1 min. In this experiment, metallic copper was added at time $t = 0$ h and, practically simultaneously, the color signals began to change. After 5 h, the signals remained constant. The experiments were conducted in a laboratory where it is difficult to avoid changes in the brightness of the ambient illumination, causing disturbances in the color signal, as can be seen in Figure 7. These disturbances were observed using the IR sensor (see the black line in the lower part of Figure 7).

In order to recreate the color using the RGB sensor values, we proceeded as follows: (1) Determine a normalization approach (i.e., into the range [0, 1]) to derive the color from the RGB color space; and (2) design a filter to correct the measured RGB data, taking into account the IR values.
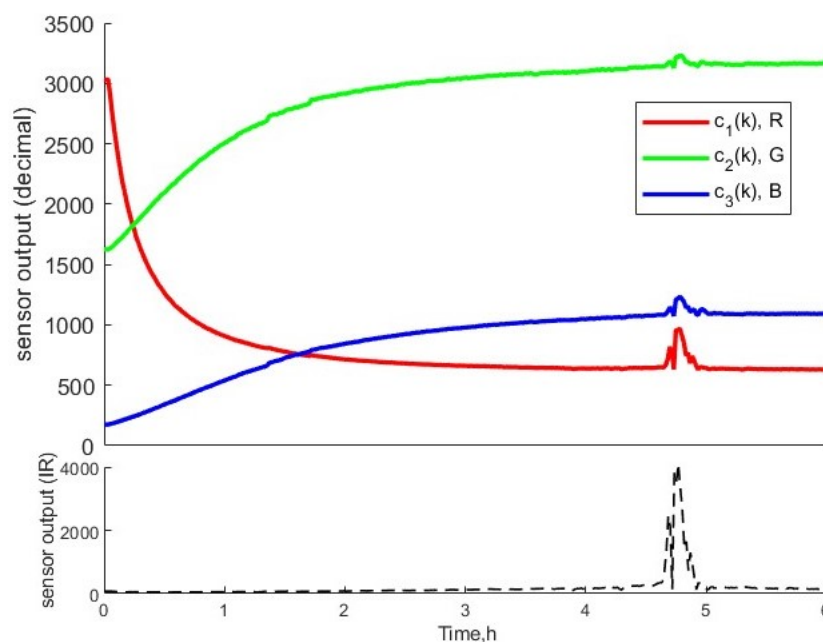
Figure 7. Raw data from RGB-IR sensor in experiment 1.

The normalization of each color component—that is, red (R), green (G), and blue (B)—into the range [0, 1] provides a simple way to achieve chromaticity invariance with respect to illumination changes, allowing the color to be derived from the RGB color space [34]. With $c_i(k)$ ($i \in 1,2,3$) denoting the measured RGB sampled value in sample k, each value is normalized using Equation (3):

$$x_i(k) = \frac{c_i(k)}{\sum\limits_{i=1}^{3} c_i(k)}, \tag{3}$$

where $y_i(k)$ corresponds to normalized RGB value, such that it satisfies the Equation (4):

$$\sum_{i=1}^{3} x_i(k) = 1. \tag{4}$$

During the experiment, we noted that the color of the liquid could not be accurately reproduced when using Equation (3) and that the sensing color was correlated with the light intensity captured by the IR sensor, as shown in Figure 8a. This was due to the light coming from the LED being reflected not only by the liquid but also the vessel's surface, as well as the intensity of the light emitted by the LED. To measure the light reflected by the vessel and the LED intensity, an experiment was conducted using water, which allowed for the determination of three weighting factors. These factors allowed us to adjust the computation of the normalized RGB values. Thus, Equation (3) was modified as follows:

$$x_i^w(k) = \frac{\alpha_i c_i(k)}{\sum\limits_{i=1}^{3} \alpha_i c_i(k)}, \tag{5}$$

where $x_i^w(k)$ are the weighted normalized RGB values in sample k; α_i are the weighting factor of values 1, 0.96 and 0.29 respectively, which were computed according to Equation (6):

$$\frac{1}{\alpha_i} = \frac{\varpi_i}{max(\varpi_1, \varpi_2, \varpi_3)}, \tag{6}$$

being $\bar{w}_i$ the mean value of the RGB signals measured in the experiment with water.

A low-pass filter, including IR measurement compensation, was designed in order to attenuate disturbances.

Figure 8a,b show RGB data processed by applying Equations (3) and (5) with a filter, respectively. It can be seen that, in the second case, the emulated color better matched the color reaction.

(a)   (b)
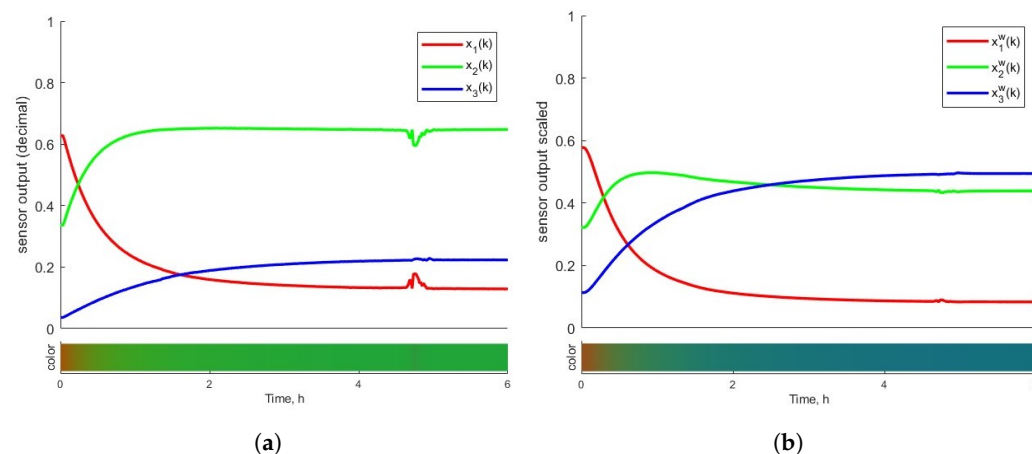
Figure 8. Processed RGB sensor data and color emulation. (**a**) Normalized using Equation (3). (**b**) Normalized using Equation (5).

2.4. Sensor Response Related Fe(III) and Cu(II) Ions Concentration

The color sensors were used with the aim of predicting the concentration of Fe(III) and Cu(II) ions present in the reaction. With this objective in mind, several experiments were carried out under identical working conditions. During these experiments, samples of the solution were taken for Fe(III) and Cu(II) analyses, following the methodology detailed in Section 2.1. Table 1 lists the result for one of these experiments. During this experiment, 11 samples were taken at time points of k_r min.

Table 1. Measured concentration of Fe(III) and Cu(II) ions using the UV-Vis and AAS absorbance, respectively, for Experiment 1.

Reaction Time (k_r), min	[Fe(III)], mg/L	[Cu(II)], mg/L
0	6134.6	0.0
5	5632.2	$\sim$ 0.0
10	5144.2	310.66
15	4915.9	514.71
25	4064.9	1063.42
35	3557.7	1405.33
45	3564.9	1622.24
75	2247.6	2348.35
105	1882.2	2577.21
195	1521.6	3081.80
225	1185.1	3081.8
345	1341.3	3250.00

The ion concentrations are plotted in Figure 9, from which it can be seen that the Fe(III) ion concentration (marked by black-star dots) followed an exponential decreasing curve similar to the red color curve, while the concentration of Cu(II) followed a logistic curve (marked by black-round dots) similar to the blue color curve, suggesting correlations between these variables. The Pearson correlation coefficient was computed to analyze the correlations between the normalized RGB sensor data processed by Equation (5) and the concentrations of Fe(III) and Cu(II) ions.
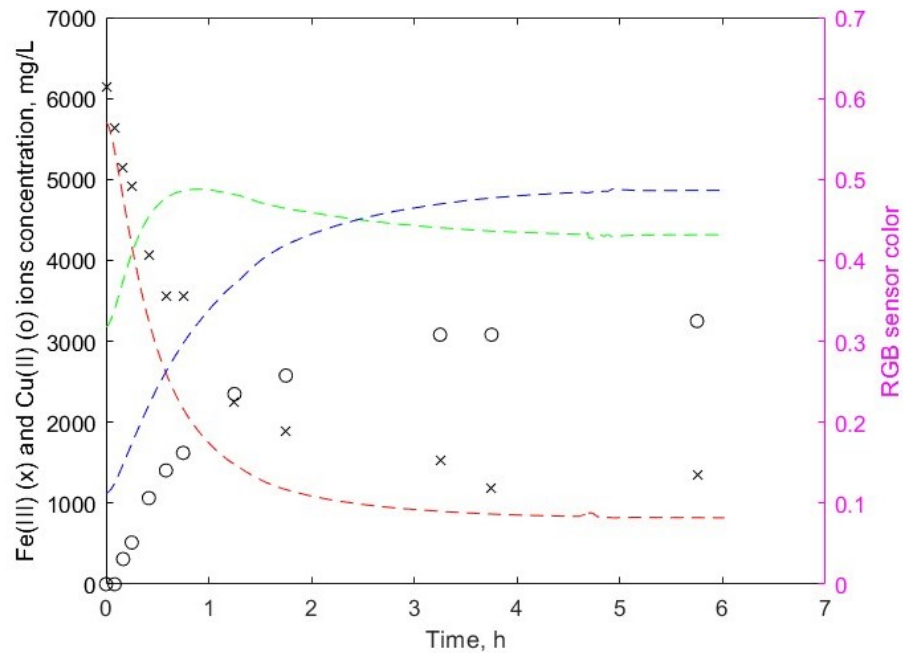
Figure 9. Fe(III) ions concentration (marked by black-star dots) and Cu(II) ions concentration (marked by black-round dots) with red, green, and blue (RGB) sensor color data.

Based on correlation analysis results, a classical linear regression was employed for model fitting. The model used in this study was defined as follows:

$$\Delta\hat{y}_{Fe}(k) = a_{11}\Delta x_i^w(k) + a_{10}, \tag{7}$$

$$\hat{y}_{Cu}(k) = a_{21}\Delta x_i^w(k) + a_{20} \tag{8}$$

where

$$\Delta\hat{y}_{Fe}(k) = \hat{y}_{Fe}(k) - y_{Fe}(0) \text{ and } \Delta x_i^w(k) = x_i^w(k) - x_i^w(0), \text{ for } i \in 1, 3,$$

a_{ij}, for $j \in 0, 1$, are the regression coefficients, y_{Fe_0} is the initial concentration of Fe(III) ions in the leaching solution, $x_i^w(k)$ are the normalized RGB sensor data computed with Equation (5), and $\hat{y}_{Fe}(k)$ and $\hat{y}_{Cu}(k)$ are the predicted concentration of Fe(III) ions and Cu(II) ions at time instant k, respectively.

To estimate the regression coefficients a_{ij}, a least squares (LS) estimation technique was used. The least squares method estimates the coefficients by minimizing the sum of squared error between the actual values ($y_{Fe}(k)$ and $y_{Cu}(k)$) and the predicted ($\hat{y}_{Fe}(k)$ and $\hat{y}_{Cu}(k)$) at each time k. As mentioned above, the actual concentrations of Fe(III) and Cu(II) were only known for some time points, k_r, which means that only a few residuals were available, leading a large variance of the regression coefficients. The method proposed for coefficient estimation and variance reduction consists of solving the least squares problem using the data from multiple experiments.

The evaluation indices selected for Fe(III) and Cu(II) ion concentration prediction verification were the coefficient of determination, R^2, and the sum of the squared error (SSE).

3. Results

3.1. Copper Percentage of PB and EC

In order to calculate the copper percentage, five wet digestions of each type of waste (i.e., PB and EC) were performed. Table 2 demonstrates that PB contained 37.5% and EC contained 22.5% of copper on average.

Table 2. Copper concentrations in PB and EC waste.

Waste Type	Sample	Copper Concentration (%)	Average Copper Concentration (%)
PB	Sample 1	34.1	37.5 ± 2.04 %
	Sample 2	38.5	
	Sample 3	37.1	
	Sample 4	39.9	
	Sample 5	38.8	
EC	Sample 1	20.8	22.5 ± 1.53 %
	Sample 2	24.8	
	Sample 3	22.0	
	Sample 4	23.2	
	Sample 5	21.8	

Stoichiometrically, according to Equation (1), at least 4.43 g of copper are required to react with 1.3 L of 6000 mg/L Fe (III) solution. To observe the whole change in color of the solution from 6000 mg/L of Fe(III) to 0 mg/L, excess copper was used in all experiments. It would not be possible to conduct a complete study of the solution's color change if copper were not present in excess. in order to ensure that there was excess copper, the experiments were carried out with a weight greater than 10% of the minimum (4.43 g); equivalent to approximately 5 g of copper. Assuming a copper content of 37.5% in PB and 22.5% in EC, 10.92 g and 18.2 g were used, respectively.

3.2. Correlation Analysis and Estimation of the Regressor Coefficients

The Pearson correlation coefficients between the concentrations of Fe(III) and Cu(II) ions and the normalized RGB sensor data are provided in Table 3. By comparing these coefficients, it can be seen that x_3^w, corresponding to the blue color, was the most highly correlated with the Fe(III) and Cu(II) ion concentrations.
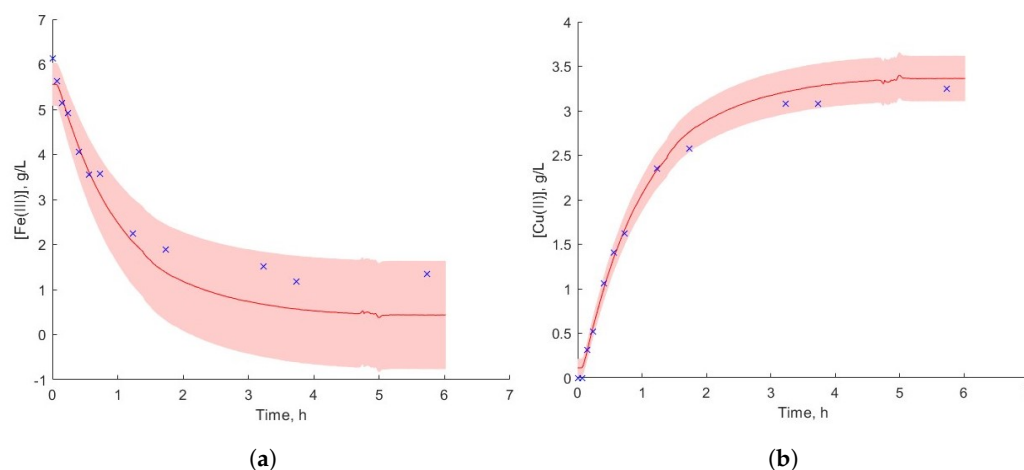
Table 3. Regression analysis.

Ions Concentration	x_1^w	x_2^w	x_3^w
Fe(III)	0.9468	0.4101	0.9741
Cu(II)	0.9603	0.3898	0.9960

The regression coefficients for Equations (7) and (8) were estimated through two experiments conducted with metallic copper. Table 4 presents the mean coefficients of the regression model, the upper and lower bounds of 95% confidence interval, and the value of the two metrics used for validation purposes (i.e., R^2 and SSE). Figure 10a,b compare the concentrations of Fe(III) and Cu(II) ions (blue-cross dots), respectively, with the simulation results obtained using the estimated coefficients. The red continuous line was computed using the mean value, while the red colored area delimits the lower and upper confidence intervals. The simulation results demonstrated that the proposed model could estimate the concentration of ions from the RGB sensor data, being more accurate in the estimation of Cu(II) ions than Fe(III) ions. The same conclusion was reached when looking at the metric performances: the copper model ($i = 2$) had a higher R^2 and lower SSE than the iron model ($i = 1$).

Table 4. Estimated parameters for the regression models adjusted for concentration of Fe(III) ($i = 2$) and Cu(II) ($i = 1$) using the least squares technique.

|	Model Coefficients		Metrics	
i	a_{i1}	a_{i0}	R^2	SSE
1	-13.68	-0.5773	0.9202	4.8645
	$(-15.61, -11.74)$	$(-1.054, -0.1011)$		
2	8.684	0.1107	0.9909	0.2199
	$(8.272, 9.096)$	$(0.0093, 0.2119)$		

(a) (b)

Figure 10. Ions concentration analyzed (blue−cross dots) and estimated (red continuous line) with bounded uncertainty (colored red area) according to the experiment using metallic copper. (**a**) Fe(III) ion concentration evolution. (**b**) Cu(II) ion concentration evolution.

*3.3. Sensor Behavior in the Presence of e-Waste*

Two types of e-waste were used to analyze the response of the RGB-IR sensor. In the case of electrical cables, the copper is coated with PVC; meanwhile, in the case of the phone boards, copper is distributed heterogeneously over the surface and integrated into the electronic components.

Figure 11a–c show the corrected data for electrical cables from the RGB-IR color sensor with color emulation, the estimated Fe(III) ion concentration, and the estimated Cu(II) ion concentration, respectively. The PVC material did not appear to interfere with the copper oxidation reaction. As can be seen from Table 5, the regression analysis, R^2, and SSE results were similar to those in previous scenarios.

The results for phone boards are shown in Figure 12a–d. Figure 12a shows the RGB raw data, while Figure 12b shows the corrected data with color emulation. Unlike the other scenarios, the signal provided by the RGB sensor was irregular, indicating that it is necessary to keep the color sensor in the same conditions throughout the duration of the experiment. We can see that, despite the irregularity of the raw data, the correction algorithm allowed for emulation of the color of the reaction. Regarding the estimation of Fe(III) and Cu(II) ion concentrations, as shown in Figure 12c,d, it was observed that the estimated model could predict the Fe(III) and Cu(II) ion concentrations with relatively good accuracy. Furthermore, from Table 5, it can be seen that the quantitative metrics were less similar, when compared with the others. Despite these observations, the model satisfactorily captured the evolution of the oxidation process.
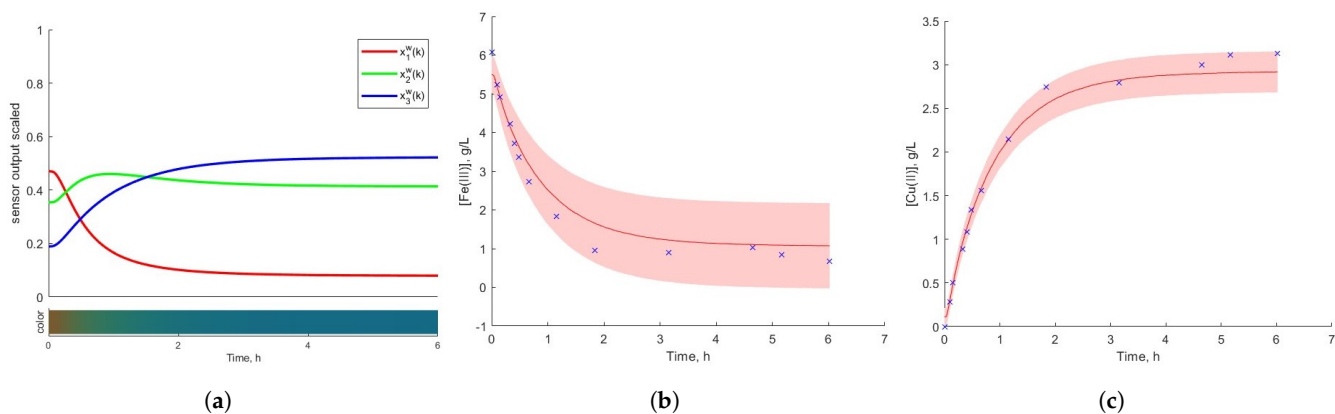
Figure 11. Data from the RGB sensor in the experiment with exp-EC. (**a**) Corrected RGB data and color emulation; (**b**) Fe(III) ion estimation; (**c**) Cu(II) ion estimation.
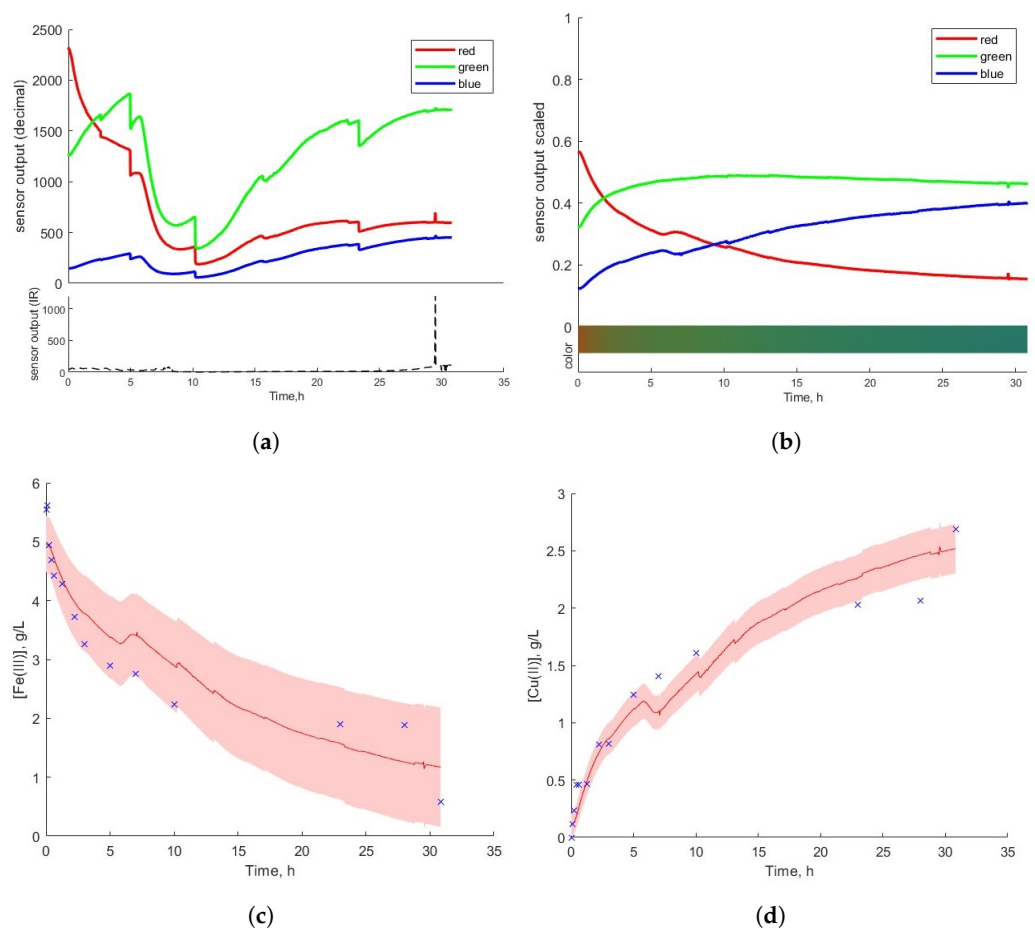
Figure 12. Data from the RGB sensor in the experiment with exp-PB. (**a**) Raw data from RGB-IR sensor. (**b**) Corrected RGB data and color emulation. (**c**) Fe(III) ions estimation evolution. (**d**) Cu(II) ions estimation evolution.

Table 5. Regression analysis for the data from experiments exp-EC and exp-PB.

Scenario	Fe(III) Ions Estimation		Cu(II) Ions Estimation	
	R^2	SSE	R^2	SSE
Exp-EC	0.7990	8.8096	0.9725	0.4314
Exp-PB	0.6781	9.6226	0.968	0.8329

4. Discussion and Conclusions

In this study, a model was developed to monitor the reduction–oxidation reaction between Fe(III) and metallic copper, as the main mechanism responsible for the biorecovery of this metal from e-waste. A device that integrates a color sensor with an Arduino and a system that allows users to collect data and track the evolution of color during the reaction were developed. This device was fixed on top of the receiver using a specially designed 3D-printed part. To proceed with the validation step, a solution containing 1.3 L of 6000 mg/L Fe(III) was prepared, to which metallic copper was added. Several samples were obtained for subsequent Cu(II) and Fe (III) analyses. The designed algorithm could satisfactorily predict the concentrations of both ions, in comparison with the results obtained experimentally, supporting the approach presented in this study. Thus, the proposed approach provides a potential tool for use as a research component to improve knowledge relevant to the use of bioprocesses for the recovery of metals from e-waste, as the amount of data supplied can be notably increased when compared with traditional analytical methods.

The signal captured by the RGB sensor was normalized using two approaches. The first—given by Equation (3)—is a conventional normalization approach, while the second case—Equation (5)—is a weighted normalization. As evidenced by the experimental data, the first model was unable to properly identify the color due to interference from the environment, including the ambient illumination, the LED intensity, and the container used for the experiment. Meanwhile, the weighted normalization approach can correct for this interference and suitably adjust the color of the solution. The weights were established by using a distilled water solution to examine the impact of the environment on the sensor data.

The concentration of Cu(II) and Fe(III) ions present in the solution were estimated using a model based on linear regression, where the variable most correlated with the concentrations of Fe(III) and Cu(II) ions was that corresponding with the blue hue, according to the correlation coefficients between the concentrations of the two ions and the colorized RGB signals. Thus, the parameters of the regression models for Fe(III) and Cu(II) were determined according to the blue color.

Two experiments were performed to assess whether the proposed concept is applicable to electronic waste: one using electric cable (where the only interference is plastic materials), and the other using PCBs (including other metals such as Ni, Mn, and Al). Similar conclusions were reached in both cases, validating both the proposed algorithm and the developed test system. In the case of electric cables, we noticed that the plastics seemed to have no effect on the color of the solution or on the rate of reaction, as the time required to oxidize the Cu(II) was comparable to that when working with pure copper. Furthermore, considering PCBs, the presence of other metals contained in the solution (10 ppm Mn and 200 ppm Ni) does not affect the color of the solution either the correspondence with the Cu (II) and Fe(III) concentrations determined by means of the RGB sensor; however, the reaction time was lengthened. Utilizing EC, Fe(III) was reduced to Fe(II) in 3 h, while working with PB extended the reaction time to 30 hours.

In summary, the proposed method can well-estimate the concentrations of Cu(II) and Fe(III) ions from the color of the solution, both when working with EC and PCBs, with Pearson coefficients equal to 0.9725 and 0.9680 for Cu(II) and equal to 0.7990 and 0.6781 for Fe (III), respectively. Therefore, it was determined that the model predicts the concentration of Cu(II) more accurately than that of Fe(III). Due to the simplicity of the matrix containing the metal, it was also noted that the proposed approach is more accurate when working with EC than with PCBs.

In conclusion, the proposed model is expected to allow scientists to keep track of the reaction between copper and iron, such that the end of the reaction may be predicted simply according to the color of the solution, without the need for trained personnel in order to take samples and perform analyses to determine the concentrations of copper and iron using AA and/or UV-VIS. This fact may result in time, energy, and cost reductions in e-waste copper biorecovery processes. The proposed technique can be rapidly and easily implemented in the context of many relevant processes. The fact that the measuring device

is not in contact with a solution that is highly acidic and oxidizing, and which contains several metals is also a key advantage. Finally, it must be remembered that the weighting factors must be adjusted beforehand, as they will differ based on the environment and the reactor where the reaction is conducted. This same approach can be also used if the leaching agent has not been produced through a biological pathway, as the biological and chemical steps are separated and the described process guarantees that biomass is not present in the solution when put into contact with e-waste.

Author Contributions: For this research article the contribution of the authors is as follows: conceptualization of the paper was done by T.E. and A.D.D.; methodology was developed by J.M., A.D.D. and A.E.; software used were provided by A.E.C.; validation of results was carried by J.M. and A.E.; formal analysis, J.M.; data curation, A.E. and T.E.; writing—original draft preparation, T.E.; writing—review and editing, T.E., A.D.D. and A.E.; project administration, A.D.D. All authors have read and agreed to the published version of the manuscript.

Data Availability Statement: The data used in this research are available upon request from the corresponding author. Datasets are published in UPCommons ResearchData, the UPC institutional repository which follows FAIR principles (Findable, Accessible, Interoperable, Reusable).

Conflicts of Interest: The authors declare that there is no conflict of interest regarding the publication of this article.

Abbreviations

The following abbreviations are used in this manuscript:

EC	Electrical cable
I2C	Iter-Integrated Circuit
IR	Infrared
LED	Light-emitting diode
LIB	Lithium batteries
LS	Least square
PB	Phone boards
PCB	Printed circuit boards
RGB	Red, Green, Blue
SSE	Sum of the square error
TIA	Transimpedance gain amplifier
UV–Vis	Ultraviolet-visible
WMP	Waste mobile phone

References

1. Forti, V.; Balde, C.P.; Kuehr, R.; Bel, G. *The Global E-Waste Monitor 2020: Quantities, Flows and the Circular Economy Potential*; United Nations University (UNU)/United Nations Institute for Training and Research (UNITAR)-co-hosted SCYCLE Programme: Bonn, Germany; International Telecommunication Union (ITU): Geneva, Switzerland; International Solid Waste Association (ISWA): Rotterdam, The Netherlands, 2020.
2. Wu, C.; Awasthi, A.K.; Qin, W.; Liu, W.; Yang, C. Recycling value materials from waste PCBs focus on electronic components: A review on technologies, obstruction and prospects. *J. Environ. Chem. Eng.* **2022**, *10*, 108516. [CrossRef]
3. Murthy, V.; Ramakrishna, S. A Review on Global E-Waste Management: Urban Mining towards a Sustainable Future and Circular Economy. *Sustainability* **2022**, *14*, 647. [CrossRef]
4. Liu, C.; Lin, J.; Cao, H.; Zhang, Y.; Sun, Z. Recycling of spent lithium-ion batteries in view of lithium recovery: A critical review. *J. Clean. Prod.* **2019**, *228*, 801–813. [CrossRef]
5. Welfens, M.J.; Nordmann, J.; Seibt, A. Drivers and barriers to return and recycling of mobile phones. Case studies of communication and collection campaigns. *J. Clean. Prod.* **2016**, *132*, 108–121. [CrossRef]
6. Gu, F.; Guo, J.; Yao, X.; Summers, P.A.; Widijatmoko, S.D.; Hall, P. An investigation of the current status of recycling spent lithium-ion batteries from consumer electronics in China. *J. Clean. Prod.* **2017**, *161*, 765–780. [CrossRef]
7. Gu, F.; Summers, P.A.; Hall, P. Recovering materials from waste mobile phones: Recent technological developments. *J. Clean. Prod.* **2019**, *237*, 117657. [CrossRef]

8. Singh, N.; Duan, H.; Yin, F.; Song, Q.; Li, J. Characterizing the materials composition and recovery potential from waste mobile phones: A comparative evaluation of cellular and smart phones. *ACS Sustain. Chem. Eng.* **2018**, *6*, 13016–13024. [CrossRef]

9. Hao, J.; Wang, Y.; Wu, Y.; Guo, F. Metal recovery from waste printed circuit boards: A review for current status and perspectives. *Resour. Conserv. Recycl.* **2020**, *157*, 104787. [CrossRef]

10. Singh, N.; Duan, H.; Ogunseitan, O.A.; Li, J.; Tang, Y. Toxicity trends in E-Waste: A comparative analysis of metals in discarded mobile phones. *J. Hazard. Mater.* **2019**, *380*, 120898. [CrossRef]

11. Petkova, M. Weekly Data: Copper Demand is Outrunning Supply. Available online: https://www.energymonitor.ai/tech/networks-grids/copper-demand-is-outrunning-supply (accessed on 3 October 2022).

12. Krishnan, S.; Zulkapli, N.S.; Kamyab, H.; Taib, S.M.; Din, M.F.B.M.; Abd Majid, Z.; Chaiprapat, S.; Kenzo, I.; Ichikawa, Y.; Nasrullah, M.; et al. Current technologies for recovery of metals from industrial wastes: An overview. *Environ. Technol. Innov.* **2021**, *22*, 101525. [CrossRef]

13. Fathima, A.; Tang, J.Y.B.; Giannis, A.; Ilankoon, I.; Chong, M.N. Catalysing electrowinning of copper from E-waste: A critical review. *Chemosphere* **2022**, *298*, 134340. [CrossRef] [PubMed]

14. Rai, V.; Liu, D.; Xia, D.; Jayaraman, Y.; Gabriel, J.C.P. Electrochemical approaches for the recovery of metals from electronic waste: A critical review. *Recycling* **2021**, *6*, 53. [CrossRef]

15. Valix, M. Bioleaching of electronic waste: Milestones and challenges. In *Current Developments in Biotechnology and Bioengineering*; Elsevier: Amsterdam, The Netherlands, 2017; pp. 407–442.

16. Rawlings, D.E. Heavy metal mining using microbes. *Annu. Rev. Microbiol.* **2002**, *56*, 65–91. [CrossRef] [PubMed]

17. Benzal, E.; Solé, M.; Lao, C.; Gamisans, X.; Dorado, A. Elemental copper recovery from e-wastes mediated with a two-step bioleaching process. *Waste Biomass Valorization* **2020**, *11*, 5457–5465. [CrossRef]

18. Benzal, E.; Cano, A.; Solé, M.; Lao-Luque, C.; Gamisans, X.; Dorado, A. Copper recovery from PCBs by Acidithiobacillus ferrooxidans: Toxicity of bioleached metals on biological activity. *Waste Biomass Valorization* **2020**, *11*, 5483–5492. [CrossRef]

19. Madriz, L.; Cabrerizo, F.M.; Vargas, R. Exploring chemical kinetics at home in times of pandemic: Following the bleaching of food dye allura red using a smartphone. *J. Chem. Educ.* **2021**, *98*, 2117–2121. [CrossRef]

20. Fernandes, G.M.; Silva, W.R.; Barreto, D.N.; Lamarca, R.S.; Gomes, P.C.F.L.; da S Petruci, J.F.; Batista, A.D. Novel approaches for colorimetric measurements in analytical chemistry–A review. *Anal. Chim. Acta* **2020**, *1135*, 187–203. [CrossRef]

21. Malkurthi, S.; Yellakonda, K.V.R.; Tiwari, A.; Hussain, A.M. Low-cost Color Sensor for Automating Analytical Chemistry Processes. In Proceedings of the 2021 IEEE Sensors, Sydney, Australia, 31 October–3 November 2021; pp. 1–4.

22. de Carvalho Oliveira, G.; Machado, C.C.S.; Inácio, D.K.; da Silveira Petruci, J.F.; Silva, S.G. RGB color sensor for colorimetric determinations: Evaluation and quantitative analysis of colored liquid samples. *Talanta* **2022**, *241*, 123244. [CrossRef]

23. Regalado, R.G.; Cruz, J.C.D. Soil pH and nutrient (nitrogen, phosphorus and potassium) analyzer using colorimetry. In Proceedings of the 2016 IEEE Region 10 Conference (TENCON), Singapore, 22–25 November 2016; pp. 2387–2391.

24. Ren, H.; Zhang, Q.; Meng, Z.; Ling, R.; Qin, W.; Wu, Z. Online monitoring strategies for colorimetric detection of cadmium ions and pH based on gold nanomaterials with a low-cost color sensor. *ACS Sustain. Chem. Eng.* **2021**, *9*, 5924–5932. [CrossRef]

25. Hasnul Hadi, M.H.; Ker, P.J.; Thiviyanathan, V.A.; Tang, S.G.H.; Leong, Y.S.; Lee, H.J.; Hannan, M.A.; Jamaludin, M.Z.; Mahdi, M.A. The amber-colored liquid: A review on the color standards, methods of detection, issues and recommendations. *Sensors* **2021**, *21*, 6866. [CrossRef]

26. Benzal-Montes, E. Study and optimisation of copper bioleaching process for electronic waste valorisation. Ph.D. Thesis, Universitat Politècnica de Catalunya (UPC), Barcelona, Spain, 2021.

27. Oktavia, B.; Lim, L.W.; Takeuchi, T. Simultaneous Determination of Fe(III) and Fe(II) Ions *via* Complexation with Salicylic Acid and 1,10-Phenanthroline in Microcolumn Ion Chromatography. *Anal. Sci.* **2008**, *24*, 1487–1492. [CrossRef] [PubMed]

28. MIKROE. COLOR 8 CLICK. 2022. Available online: https://www.mikroe.com/color-8-click (accessed on 2 February 2022).

29. MIKROE. LED DRIVER 2 CLICK. 2022. Available online: https://www.mikroe.com/led-driver-2-click (accessed on 2 February 2022).

30. DFROBOT. pH Meter. Available online: https://wiki.dfrobot.com/PH_meter_SKU__SEN0161_k (accessed on 2 February 2022).

31. Nusairat, J.F. Sense HAT. In *Rust for the IoT: Building Internet of Things Apps with Rust and Raspberry Pi*; Apress: Berkeley, CA 2020; pp. 429–481.

32. BH1749NUC. Digital 16bit Serial Output Type Color Sensor IC. 2017. Available online: https://fscdn.rohm.com/en/products/databook/datasheet/ic/sensor/light/bh1749nuc-e.pdf (accessed on 2 February 2022).

33. CREE. XLamp XP-E2 LED. Available online: https://assets.cree-led.com/a/ds/x/XLamp-XPE2.pdf (accessed on 2 February 2022).

34. Vertan, C.; Boujemaa, N. Color texture classification by normalized color space representation. In Proceedings of the Proceedings 15th International Conference on Pattern Recognition, ICPR-2000, Barcelona, Spain, 3–7 September 2000; Volume 3, pp. 580–583.